

Tuning Catalytic Efficiency: Thermodynamic Optimization of Zr-Doped Ti_3C_2 and Ti_3CN MXenes for HER Catalysis

Shrestha Dutta and Rudra Banerjee

Department of Physics and Nanotechnology, SRM Institute of Science and Technology, Kattankulathur, Tamil Nadu, 603203, India

(*rudrab@srmist.edu.in)

(Dated: January 28, 2025)

Hydrogen production via the Hydrogen Evolution Reaction (HER) is critical for sustainable energy solutions, yet the reliance on expensive platinum (Pt) catalysts limits scalability. Zirconium-doped (Zr-doped) MXenes, such as Ti_3C_2 and Ti_3CN , emerge as transformative alternatives, combining abundance, tunable electronic properties, and high catalytic potential. Using first-principles density functional theory (DFT), we show that Zr doping at 3% and 7% significantly enhances HER activity by reducing the work function to the optimal range of 3.5-4.5 eV and achieving near-zero Gibbs free energy ($|\Delta G_{H^*}|$) values of 0.18-0.16 eV, conditions ideal for efficient hydrogen adsorption and desorption. Bader charge analysis reveals substantial charge redistribution, with enhanced electron accumulation at Zr and N sites, further driving catalytic performance. This synergy between optimized electronic structure and catalytic properties establishes Zr-doped MXenes as cost-effective, high-performance alternatives to noble metals for HER. By combining exceptional catalytic efficiency with scalability, our work positions Zr-doped MXenes as a breakthrough for green hydrogen production, offering a robust pathway toward renewable energy technologies and advancing the design of next-generation non-precious metal catalysts.

I. INTRODUCTION

The increasing global demand for energy, driven by industrial growth and population expansion, necessitates the urgent development of sustainable and eco-friendly energy solutions [1, 2]. Hydrogen, as a clean and renewable energy carrier, has emerged as a promising solution to these challenges, aligning with global sustainability goals [3, 4]. Among the various hydrogen production methods, the Hydrogen Evolution Reaction (HER), which relies on water splitting, has gained attention due to its cost-effectiveness and environmental benefits [5, 6]. The HER process efficiently produces hydrogen gas with water as a renewable source and oxygen (O_2) as the sole byproduct, making it an attractive route for green energy conversion [7].

Electrocatalysts are pivotal to HER efficiency, accelerating the reaction kinetics and reducing energy barriers [5]. Precious metal-based catalysts such as platinum (Pt) and ruthenium (Ru) are widely regarded for their superior catalytic performance, achieving low overpotentials and high cathodic current densities [8, 9]. However, the scarcity and prohibitive costs of these materials pose significant obstacles to their large-scale deployment, emphasizing the need for cost-effective alternatives [10, 11]. As a result, extensive research efforts are directed towards non-precious metal (NPM)-based electrocatalysts, which offer the potential to balance performance and cost [12–14].

Despite the progress made in NPM-based catalysts, chal-

lenges remain in optimizing their electrical conductivity and long-term stability in aqueous environments, which are critical to maintaining high catalytic activity and durability [15–17]. Various classes of NPM-based catalysts, such as transition metal dichalcogenides (TMDs) [18], metal nitrides [19], and carbon-based materials like MXenes [20], have been explored for HER applications. Among these, MXenes—two-dimensional (2D) transition metal carbides, nitrides, and carbonitrides—stand out for their promising catalytic properties, including excellent electrical conductivity, large surface areas [21, 22], and tunable electronic structures [23].

MXenes, represented by the general formula $M_{n+1}X_nT_x$, where M is a transition metal and X is carbon or nitrogen, possess surface terminations such as $-F$, $-O$, or $-OH$ [24–26]. These materials have demonstrated high potential for HER due to their multiple active sites, robust mechanical properties, and hydrophilicity, which help their interaction with water molecules [27, 28]. Moreover, the tunability of their Fermi levels enhances their catalytic activity in HER by improving electron transfer efficiency [29, 30]. Nevertheless, the catalytic performance of MXenes in HER is primarily governed by the Gibbs free energy of hydrogen adsorption (ΔG_{H^*}), with an optimal value close to zero being desirable for efficient hydrogen adsorption and desorption during the reaction [16, 22, 31, 32].

In addition to $|\Delta G_{H^*}|$, the work function (ϕ), defined as “the work needed to move an electron from a surface to a point in vacuum sufficiently far away from this surface

[33] has also emerged as a good catalytic descriptor in recent time [34, 35]. The value of ϕ too less ($\leq 3\text{eV}$) or too high ($\geq 6\text{eV}$) hinders either the Volmer or the Heyrovsky/Tafel kinematics. The "habitable zone" of the ϕ is found out to be in the range of 3.5-4.5eV [34, 36].

Titanium carbide-based MXenes Ti_3C_2 have garnered significant attention as potential catalysts for the hydrogen evolution reaction (HER) due to their tunable electronic structure, high surface area, and excellent hydrophilicity [37, 38]. However, their catalytic performance is limited by several shortcomings, including sub-optimal hydrogen adsorption energy $|\Delta G_{\text{H}^*}|$, insufficient active site density, and sluggish electron transfer kinetics [39]. The metallic nature of Ti_3C_2 often leads to hydrogen adsorption that is either too strong or too weak, which hinders the HER process. Additionally, the surface terminations typically present on Ti_3C_2 , such as $-\text{OH}$, $-\text{F}$, and $-\text{O}$, introduce localized electronic states that are unfavorable for catalytic activity, thereby increasing the overpotential and reducing turnover frequency [40, 41].

Doping has emerged as a promising strategy to address these limitations by modulating the electronic properties and surface chemistry of Ti_3C_2 . Transition metal doping (e.g., Fe, Co, or Ni) can adjust the d -band center of Ti_3C_2 , optimizing $|\Delta G_{\text{H}^*}|$ and enhancing its catalytic activity [42]. Non-metal doping, such as nitrogen or boron, can further enhance charge redistribution and stabilize defect states, thereby improving electron transfer [31]. For instance, Ni-doped Ti_3C_2 has demonstrated significantly reduced overpotential and enhanced HER efficiency due to improved hydrogen adsorption and charge transport properties [42, 43].

In this context, our study explores Zr-doped Ti-based MXenes as potential HER catalysts, aiming to overcome the limitations of pristine Ti_3C_2 and Ti_3CN monolayers. By introducing Zr dopants at concentrations of 3% and 7%, we investigate the impact of doping on the electronic structure, catalytic activity, and $|\Delta G_{\text{H}^*}|$ values of these MXenes. Additionally, we examine the effects of hydrogen coverage on unterminated MXene monolayers to further elucidate the catalytic mechanisms. Our results demonstrate that Zr-doping can significantly enhance the HER catalytic performance of Ti-based MXenes, offering a pathway towards the development of cost-effective and efficient electrocatalysts for sustainable hydrogen production.

II. COMPUTATIONAL DETAILS

All calculations were performed within the framework of density functional theory (DFT) [44] using the projector-augmented wave (PAW) method [45], as implemented in the Vienna *Ab-initio* Simulation Package (VASP) [46–49]. The exchange-correlation effects were treated using the Perdew-Burke-Ernzerhof (PBE) functional under the generalized gradient approximation (GGA) [50]. To ensure the accurate representation of valence electron-ion interactions, the plane-wave pseudopotential approach was employed, with a plane-wave cutoff energy set to 520 eV.

The primary focus of this work was on monolayer Ti-based MXenes, both in pristine and Zr-doped configurations. A vacuum layer of approximately 16 Å was introduced along the z -axis to eliminate spurious interactions between periodic images of the layers. For structural relaxations, a convergence criterion of 1.0×10^{-3} eV/Å was adopted, ensuring precise ionic positions.

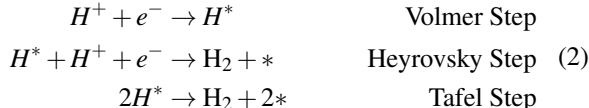
A Γ -centered Monkhorst-Pack [51] k -point mesh of $14 \times 14 \times 2$ was used for the MXene unit cell, with an equivalent k -point density applied to $3 \times 3 \times 1$ supercells. The choice of this k -point sampling ensured adequate Brillouin zone integration for both pristine and doped systems. To capture the strong Coulombic interactions in the d -orbitals, the Hubbard U correction was applied using $U_{\text{eff}} = 3.0$ eV for Ti [52] and $U_{\text{eff}} = 2.85$ eV for Zr [53]. The total energy minimization and convergence of force components were carefully monitored to ensure high accuracy in all simulations.

The thermodynamic stability of the MXene structures was evaluated by calculating the formation energy (FE) using the standard expression:

$$FE(\text{M}_3\text{C}_2) = E(\text{M}_3\text{C}_2) - 3\mu_{\text{M}} - 2\mu_{\text{C}}, \quad (1)$$

where $E(\text{M}_3\text{C}_2)$ represents the total energy of the MXene compound, and μ_{M} and μ_{C} are the chemical potentials of the metal and carbon atoms respectively, in their standard reference states.

The Volmer-Heyrovsky or the Volmer-Tafel reaction path of the HER ($2\text{H}^+ + 2\text{e}^- \rightarrow \text{H}_2$)



is largely controlled by the free energy of H absorption, or the Gibbs free energy (ΔG_{H^*}) [22, 31]. The necessary but insufficient condition for a material as "good" HER

catalyst is $|\Delta G_{H^*}| \approx 0$. The free energy change for the intermediate H^* adsorption state is given by:

$$\begin{aligned} \Delta G_{H^*} &= \Delta E_{H^*} + \Delta ZPE_{H^*} - T\Delta S_{H^*} \\ \Delta E_{H^*} &= E_{\text{Layer}+H^*} - E_{\text{Layer}} - \frac{1}{2}E_{H_2}, \end{aligned} \quad (3)$$

where ΔE_{H^*} is the adsorption energy of hydrogen, $E_{\text{Layer}+H^*}$ and E_{Layer} represent the total energies of the hydrogen-adsorbed and clean MXene surfaces, respectively, and E_{H_2} is the total energy of molecular hydrogen in the gas phase.

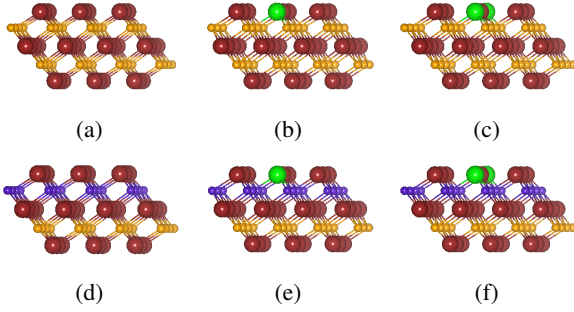


FIG. 1: Monolayer structures of (a) Ti_3C_2 ; (b) $(Ti_{0.97}Zr_{0.03})_3C_2$; (c) $(Ti_{0.93}Zr_{0.07})_3C_2$; (d) Ti_3CN ; (e) $(Ti_{0.97}Zr_{0.03})_3CN$; and (f) $(Ti_{0.93}Zr_{0.07})_3CN$. Ti, Zr, C and N atoms are depicted as maroon, green, orange and violet balls, respectively.

The zero-point energy correction (ΔZPE_{H^*}) accounts for the quantum vibrational effects of the adsorbed hydrogen atom, with values ranging from 0.01 to 0.04 eV for metal surfaces[54]. ($T\Delta S_{H^*}$), approximately 0.4 eV at room temperature, reflects the entropy difference between the adsorbed hydrogen and the gas-phase H_2 molecule [55, 56]. Based on Nørskov's volcano plot, optimal HER catalysts exhibit $|\Delta G_{H^*}| \leq 0.3$ eV [55], a criterion we employed to identify promising electrocatalysts.

The work function has been calculated using

$$\phi = e\phi_{\text{vacuum}} - E_F$$

where ϕ_{vacuum} is the potential far away from the surface.

III. RESULTS AND DISCUSSION

FIG. (1) shows the schematic of the doped and undoped structures used in this study. FIG. (1a) and FIG. (1d) shows the Ti_3C_2 and Ti_3CN structures respectively. FIG. (1b) and FIG. (1c) are showing 0.3% and 0.7%

doping of Zr at Ti site of Ti_3C_2 (Those structures will be referred as TZ_3C and TZ_7C for brevity in the rest of this manuscript). FIG. (1e) and FIG. (1f) are showing 0.3% and 0.7% doping of Zr at Ti site of Ti_3CN , and will be referred as TZ_3CN and TZ_7CN in the rest of the manuscript. All the doped systems are found to be thermodynamically stable (2nd column of table (I)). Note that increased Zr doping in Ti_3C_2 makes the system unstable, but due to higher electronegativity of N compared to C, Zr doped Ti_3CN shows the increase in stability. The result aligns with the reported energy above the hull values of 0.05 eV/atom for Ti_3C_2 [57] and 0.02 eV/atom for Zr_3N_2 [58], indicating enhanced stability of the Zr-doped system.

The catalytic performance of each of the above systems are evaluated through calculations of the $|\Delta G_{H^*}|$ as discussed above. FIG. (2a) shows the $|\Delta G_{H^*}|$ of the systems studied. The results shows systematic decrease of $|\Delta G_{H^*}|$ with higher concentrations of Zr. For pristine Ti_3C_2 , the ΔG_{H^*} value is 1.510 eV, while Ti_3CN shows a slightly lower value of 1.251 eV, both of which indicate suboptimal HER activity. In contrast, the introduction of Zr into the MXene lattice significantly reduces $|\Delta G_{H^*}|$, with TZ_7C and TZ_7CN exhibiting values of 0.185 eV and 0.160 eV, respectively. These values are remarkably close to the ideal range for HER, suggesting that Zr-doping dramatically enhances the catalytic efficiency of the MXenes. The values are tabulated in table (I) for comparison.

To elucidate the origin of the significant reduction in $|\Delta G_{H^*}|$ observed with Zr doping, we performed comprehensive electronic structure calculations to determine the work function (ϕ) and Bader charge distribution. The work function is a critical parameter in determining the efficiency of materials for the HER. FIG. (2b) shows the ϕ with respect to the surface. We observe significant variations in ϕ with doping concentration. The pristine MXenes, Ti_3C_2 and Ti_3CN , exhibit relatively higher work functions, limiting their HER performance. Upon doping with 3% Zr, i.e. TZ_3C and TZ_3CN , show reduced work functions, nearing the optimal range, suggesting enhanced catalytic activity. Increasing the Zr content to 7% in TZ_7C and TZ_7CN further takes the work function squarely within the desired range. This systematic change demonstrates that Zr doping effectively tunes the electronic properties of MXenes, enhancing their HER efficiency. Furthermore, the correlation between $|\Delta G_{H^*}|$ and the work function, illustrated in FIG. (2c), reveals a robust linear relationship, underscoring the direct impact of electronic structure modifications on catalytic performance. These findings align with prior studies that have demonstrated a strong link between the electronic properties of MXenes and their catalytic

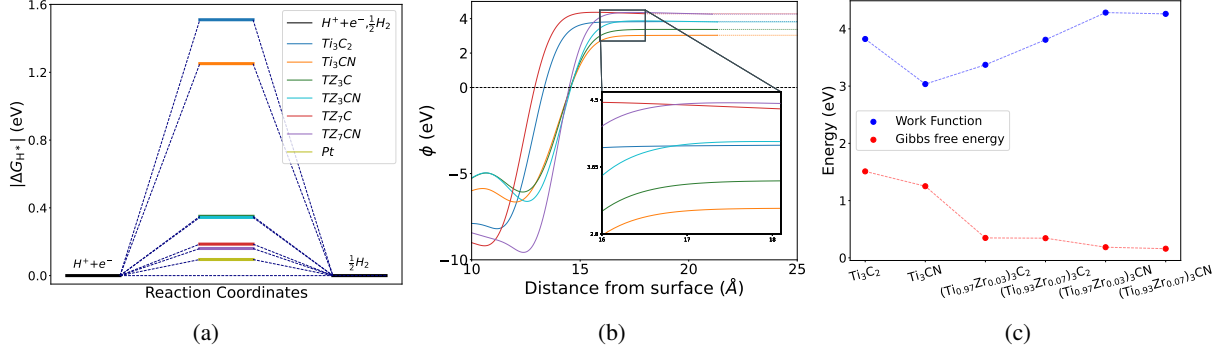


FIG. 2: (a) $|\Delta G_{H^*}|$ for the MXene systems studied, with reference to Pt; (b) calculated work function normal to the surface. The dotted part of each curves are the constant line for comparison, and not actually calculated. Inset shows the zoomed in figure for better visualization. The line color indicates same systems as in (a); and (c) correlation between ϕ and $|\Delta G_{H^*}|$.

activity[41]. The observed trend suggests that Zr doping not only tunes the electronic environment but also optimizes the catalytic properties of the material, making Zr-doped Ti-based MXenes a promising candidates for HER applications.

We systematically investigated the electronic structure of pristine and Zr-doped Ti_3C_2 to elucidate the correlation between their electronic properties and catalytic performance in the hydrogen evolution reaction (HER). Pristine Ti_3C_2 , a well-studied MXene, exhibits high electrical conductivity due to its metallic nature, characterized by a substantial density of states (DOS) near the Fermi level, as shown in FIG. (3a). The layered structure of Ti_3C_2 helps efficient electron mobility, a critical factor for enhancing catalytic reactions. Likewise, Ti_3CN , which has mixed carbon and nitrogen occupancy at the X-sites, demonstrates comparable electronic behavior (FIG. (3d)). These results are consistent with earlier DFT studies that have highlighted the metallic character of pristine MXenes and their capacity for electron transfer in various catalytic contexts [59, 60]. Introducing Zr atoms into the MXene structure at 3% and 7% concentrations induces notable changes in the electronic structure. The DOS of the Zr-doped MXenes (Figure 3(b,c,e,f)) shows an increase in electronic states near the Fermi level, particularly between -0.5 eV and -3.0 eV. This increase is attributed to Zr's larger electron affinity compared to Ti, resulting in enhanced electron donation. The higher DOS at the Fermi level for the Zr-doped structures indicates a greater availability of electrons, which is critical for promoting catalytic reactions. These additional states effectively lower the energy barrier for electron transfer to adsorbed hydrogen ions (H^+), thereby facilitating HER [61].

MXenes	E_{form} (eV/f.u.)	$ \Delta G_{H^*} $ (eV)	Bond lengths(\AA)			
			Ti-C	Zr-C	Ti-N	Zr-N
Ti_3C_2	-11.80	1.51 ^(0.927) [40]	2.09	-	-	-
Ti_3CN	-9.24	1.25 ^(0.770) [41]	2.10	-	2.09	-
TZ_3C	-1.30	0.35	2.10	2.23	-	-
TZ_7C	-1.07	0.34	2.11	2.23	-	-
TZ_3CN	-0.78	0.19	2.08	-	2.07	2.25
TZ_7CN	-1.71	0.16	2.08	-	2.07	2.23

TABLE I: Formation energies (E_{form}), Gibbs free energies $|\Delta G_{H^*}|$ for hydrogen adsorption on surfaces, and the bond lengths of pristine and Zr-doped MXenes. The value in the brackets are the experimental values obtained by other groups. The values differ primarily due to the choice of terminators and the choice PBE potentials.

FIG. (4) illustrates the Bader charge analysis for four MXene systems. The pristine Ti_3C_2 (FIG. (4a)) shows low charge accumulation of Ti and C atoms. In contrast, Zr doping, where $|\Delta G_{H^*}|$ is reduced to ≈ -0.1 eV, accumulates large charge on the Zr and N atoms, as shown in TZ_3C (FIG. (4b)) and TZ_7CN (FIG. (4d)). Ti_3CN , TZ_3C and TZ_3CN shows the similar trend of higher charge accumulation in Zr and N compared to Ti and C and results in lower $|\Delta G_{H^*}|$.

The enhanced catalytic performance of Zr-doped MXenes can be attributed to the synergistic role of Zr and N. Zr, with its higher electron affinity compared to Ti, facilitates greater charge redistribution within the lattice, increasing surface electron availability crucial for HER. N, being more electronegative than C, stabilizes hydro-

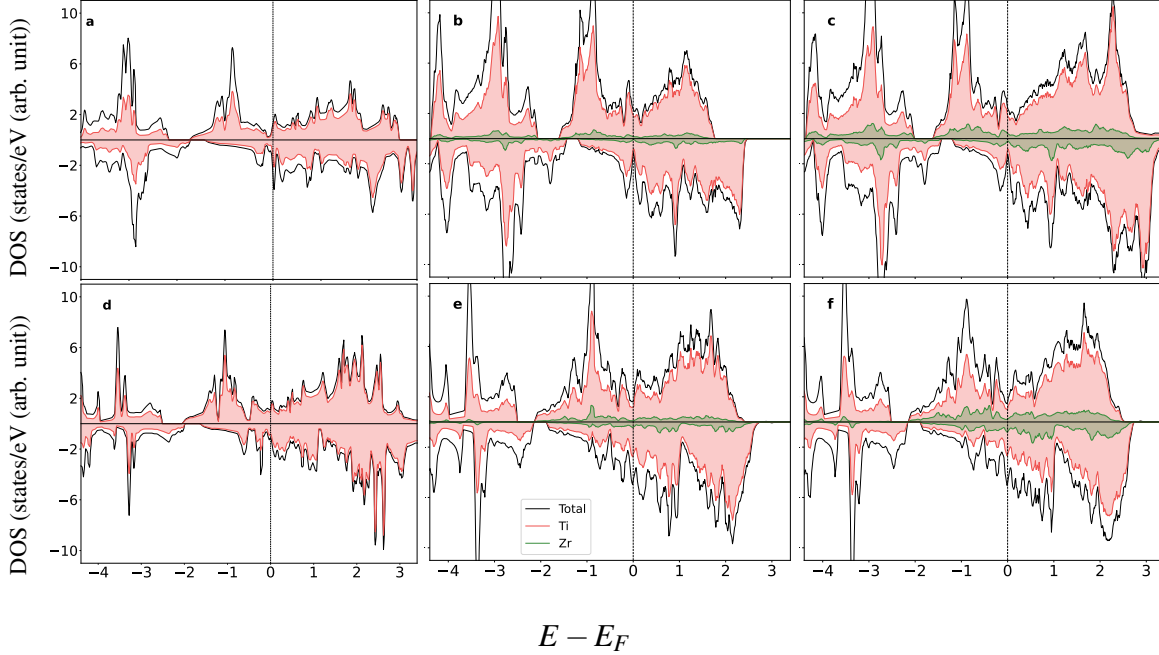


FIG. 3: Calculated total DOS of monolayer (a) Ti_3C_2 , (b) $(\text{Ti}_{.97}\text{Zr}_{.03})_3\text{C}_2$, (c) $(\text{Ti}_{.93}\text{Zr}_{.07})_3\text{C}_2$, (d) Ti_3CN , (e) $(\text{Ti}_{.97}\text{Zr}_{.03})_3\text{CN}$, and (f) $(\text{Ti}_{.93}\text{Zr}_{.07})_3\text{CN}$ using Hubbard parameter U ($U = 3.0$ for Ti and $U = 2.85$ for Zr).

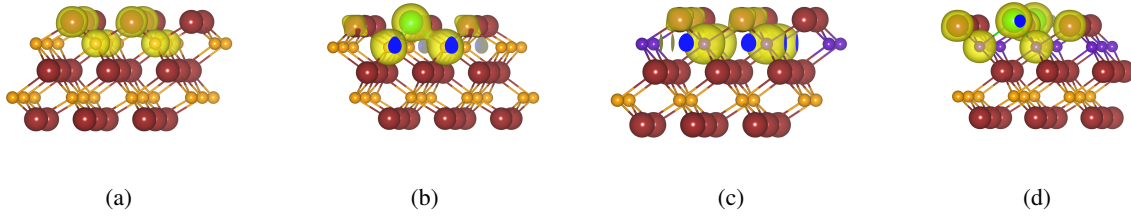


FIG. 4: Charge density distribution in (a) Ti_3C_2 ; (b) TZ_3C ; (c) Ti_3CN (d) TZ_7CN . Ti, Zr, C and N atoms are depicted as maroon, green, orange and violet balls, respectively.

gen adsorption by modifying the local electronic environment. This combination fine-tunes the Gibbs free energy and provides more favorable adsorption sites for H^* intermediates.

In summary, our results reveal that Zr-doping of Ti_3C_2 and Ti_3CN MXenes significantly enhances their catalytic performance for HER by modifying the electronic structure and reducing the Gibbs free energy of hydrogen adsorption. The improved electron mobility and increased surface electron density, along with the lowered work function, contribute to the superior catalytic efficiency of the Zr-doped MXenes. These findings highlight the potential of Zr-doped MXenes as promising candidates for sustainable hydrogen production, rivalling the perfor-

mance of traditional platinum-based catalysts.

IV. CONCLUSION

Our study demonstrates the significant catalytic potential of Zr-doped Ti-based MXenes for the hydrogen evolution reaction (HER). Specifically, the Zr-doped single-layered MXenes $(\text{Ti}_{.97}\text{Zr}_{.03})_3\text{C}_2$ and $(\text{Ti}_{.97}\text{Zr}_{.03})_3\text{CN}$ exhibit ΔG_{H^*} values around 0.3 eV, while higher Zr concentrations, as seen in $(\text{Ti}_{.93}\text{Zr}_{.07})_3\text{C}_2$ and $(\text{Ti}_{.93}\text{Zr}_{.07})_3\text{CN}$, result in optimal values of 0.18 and 0.16 eV, respectively. These near-zero ΔG_{H^*} values indicate that Zr-doped MXenes, particularly at higher doping levels, have excellent hydrogen adsorption properties, approaching the cat-

alytic efficiency of platinum-based catalysts.

Our density of states (DOS) analysis confirms that Zr doping enhances the metallic character and increases the electron density near the Fermi level, which is pivotal for efficient electron transfer during HER. The improved electronic properties directly translate into enhanced catalytic activity, as demonstrated by the reduction in ΔG_{H^*} and lower work functions observed in the doped structures. This enhanced electron mobility and surface electron density, driven by Zr's introduction, significantly reduces the energy barrier for hydrogen adsorption, thereby facilitating HER.

An important distinction in our study is the focus on unterminated MXenes, a departure from the majority of existing literature, which primarily investigates MXenes with surface terminations such as $-O$, $-OH$, or $-F$. While surface terminations are often considered to stabilize MXenes and enhance their chemical reactivity, they introduce complexity that can obscure the intrinsic properties of the material. By studying unterminated MXenes, we isolate the electronic and catalytic behaviors of the pristine 2D structures, providing a clearer understanding of their core material properties. This approach allows for an evaluation of the impact of Zr doping on the electronic structure and catalytic activity, particularly in the context of hydrogen evolution reactions (HER). Furthermore, insights gained from unterminated MXenes form a crucial baseline for future studies, facilitating a deeper comprehension of how surface functionalization affects performance. Thus, our study offers a more fun-

damental exploration of MXene chemistry, which is essential for designing next-generation HER catalysts.

These findings underscore the potential of Zr-doped Ti-based MXenes as highly efficient and cost-effective alternatives to noble metal catalysts for hydrogen production. The ability to tailor the electronic structure through controlled doping opens new pathways for optimizing 2D MXenes for energy conversion technologies. This study paves the way for experimental validation and further exploration of Zr-doped MXenes in sustainable hydrogen production via water splitting, offering a promising avenue for green energy applications. Future work could focus on the experimental validation of Zr-doped Ti-based MXenes to confirm the theoretical predictions. Exploring other dopants, their synergetic effects, and the influence of surface terminations under different environmental conditions would provide deeper insights into optimizing HER activity. Additionally, integrating machine learning techniques to identify optimal compositions could accelerate the discovery of efficient catalysts for sustainable hydrogen production.

ACKNOWLEDGMENTS

We express our sincere gratitude to the high performance computing center (HPCC), SRMIST and the Department of Physics and Nanotechnology for their support of the computational facility. We are appreciative of the computational resource provided by the National Param supercomputing facility (NPSF, CDAC), Government of India. We also express our heartiest gratitude to Selective Excellence Research Initiative (SERI), SRMIST for their support in our research work.

-
- [1] Z. W. Seh, J. Kibsgaard, C. F. Dickens, I. Chorkendorff, J. K. Nørskov, and T. F. Jaramillo, Combining Theory and Experiment in Electrocatalysis: Insights into Materials Design, *Science* **355**, eaad4998 (2017).
 - [2] S. Chu and A. Majumdar, Opportunities and Challenges for a Sustainable Energy Future, *Nature* **488**, 294 (2012).
 - [3] G. Glenk and S. Reichelstein, Reversible Power-to-Gas Systems for Energy Conversion and Storage, *Nature Communications* **13**, 2010 (2022).
 - [4] L. Fan, Z. Tu, and S. H. Chan, Recent Development of Hydrogen and Fuel Cell Technologies: A Review, *Energy Reports* **7**, 8421 (2021).
 - [5] S. Wang, A. Lu, and C.-J. Zhong, Hydrogen Production from Water Electrolysis: Role of Catalysts, *Nano Convergence* **8** (2021).
 - [6] Z. Chen, X. Duan, W. Wei, S. Wang, and B.-J. Ni, Recent Advances in Transition Metal-based Electrocatalysts for Alkaline Hydrogen Evolution, *J. Mater. Chem. A* **7**, 14971 (2019).
 - [7] M. Khan, H. Zhao, W. Zou, Z. Chen, W. Cao, J. Fang, L. Zhang, and J. Zhang, Recent Progresses in Electrocatalysts for Water Electrolysis, *Electrochemical Energy Reviews* **1** (2018).
 - [8] J. N. Hansen, H. Prats, K. K. Toudahl, N. Mørch Secher, K. Chan, J. Kibsgaard, and I. Chorkendorff, Is There Anything Better than Pt for HER?, *ACS Energy Letters* **6**, 1175 (2021).
 - [9] W. Luo, Y. Wang, and C. Cheng, Ru-based Electrocatalysts for Hydrogen Evolution Reaction: Recent Research Advances and Perspectives, *Materials Today Physics* **15**, 100274 (2020).
 - [10] C. Li and J.-B. Baek, Recent Advances in Noble Metal (Pt, Ru, and Ir)-Based Electrocatalysts for Efficient Hydrogen Evolution Reaction, *ACS Omega* **5**, 31 (2020).
 - [11] L. Zhang, J. Zhang, J. Fang, X.-Y. Wang, L. Yin, W. Zhu, and Z. Zhuang, Cr-Doped CoP Nanorod Arrays as High-Performance Hydrogen Evolution Reaction Catalysts at High Current Density, *Small* **17**, 2100832 (2021).

- [12] H. Mistry, S. Varela, Ana Sofia, P. Strasser, and B. R. Cuenya, Nanostructured Electrocatalysts with Tunable Activity and Selectivity, *Nature Reviews Materials* **1**, 16009 (2016).
- [13] A. Jayakumar, R. P. Antony, R. Wang, and J.-M. Lee, MOF-Derived Hollow Cage Ni_xCo_{3-x}O₄ and Their Synergy with Graphene for Outstanding Supercapacitors, *Small* **13**, 1603102 (2017).
- [14] J. Anjali, V. K. Jose, and J.-M. Lee, Carbon-based Hydrogels: Synthesis and their Recent Energy Applications, *J. Mater. Chem. A* **7**, 15491 (2019).
- [15] X. Peng, C. Pi, X. Zhang, S. Li, K. Huo, and P. K. Chu, Recent Progress of Transition Metal Nitrides for Efficient Electrocatalytic Water Splitting, *Sustainable Energy Fuels* **3**, 366 (2019).
- [16] S. Bai, M. Yang, J. Jiang, X. He, J. Zou, Z. Xiong, G. Liao, and S. Liu, Recent Advances of MXenes as Electrocatalysts for Hydrogen Evolution Reaction, *npj 2D Materials and Applications* **78** (2021).
- [17] S. Zhang, X. Zhang, Y. Rui, R. Wang, and X. Li, Recent Advances in Non-precious Metal Electrocatalysts for pH-universal Hydrogen Evolution Reaction, *Green Energy and Environment* **6**, 458 (2021).
- [18] L. Wu and J. P. Hofmann, Comparing the Intrinsic HER Activity of Transition Metal Dichalcogenides: Pitfalls and Suggestions, *ACS Energy Letters* **6**, 2619 (2021).
- [19] R. Jamil, R. Ali, S. Loomba, J. Xian, M. Yousaf, K. Khan, B. Shabbir, C. F. McConville, A. Mahmood, and N. Mahmood, The Role of Nitrogen in Transition-metal Nitrides in Electrochemical Water Splitting, *Chem Catalysis* **1**, 802 (2021).
- [20] L. Zhang, J. Xiao, H. Wang, and M. Shao, Carbon-Based Electrocatalysts for Hydrogen and Oxygen Evolution Reactions, *ACS Catalysis* **7**, 7855 (2017).
- [21] R. Gautam, N. Marriwala, and R. Devi, A Review: Study of Mxene and Graphene together, *Measurement: Sensors* **25**, 100592 (2023).
- [22] X. Li, Y. Bai, X. Shi, N. Su, G. Nie, R. Zhang, H. Nie, and L. Ye, Applications of MXene (Ti₃C₂T_x) in Photocatalysis: A Review, *Mater. Adv.* **2**, 1570 (2021).
- [23] J. Hart, K. Hantanasirisakul, A. Lang, B. Anasori, D. Pinto, Y. Pivak, J. Ommé, S. May, Y. Gogotsi, and M. Taheri, Control of MXenes' Electronic Properties through Termination and Intercalation, *Nature Communications* **10** (2019).
- [24] M. Naguib, V. N. Mochalin, M. W. Barsoum, and Y. Gogotsi, 25th Anniversary Article: MXenes: A New Family of Two-Dimensional Materials, *Advanced Materials* **26**, 982 (2014).
- [25] M. Khazaei, M. Arai, T. Sasaki, M. Estili, and M. Saito, Novel electronic and magnetic properties of two-dimensional transition metal carbides and nitrides, *Physical Chemistry Chemical Physics* **16**, 7841 (2014).
- [26] M. Ghidui, M. R. Lukatskaya, M. Zhao, Y. Gogotsi, and M. W. Barsoum, Conductive two-dimensional titanium carbide 'clay' with high volumetric capacitance, *Nature* **516**, 78 (2015).
- [27] S. I. Yengejeh, S. A. Kazemi, W. Wen, and Y. Wang, Oxygen-terminated M₄X₃ MXenes with Superior Mechanical Strength, *Mechanics of Materials* **160**, 103957 (2021).
- [28] B. Wyatt, A. Rosenkranz, and B. Anasori, Two-dimensional MXenes: Tunable Mechanical and Tribological Properties, *Advanced Materials* **33**, 2007973 (2021).
- [29] Y. Gogotsi and Q. Huang, MXenes: Two-Dimensional Building Blocks for Future Materials and Devices, *ACS Nano* **15**, 5775 (2021).
- [30] I. Ashraf, S. Ahmad, F. Nazir, D. Dastan, Z. Shi, H. Garmestani, and M. Iqbal, Hydrothermal synthesis and water splitting application of d-ti₃c₂ mxene/v₂o₅ hybrid nanostructures as an efficient bifunctional catalyst, *International Journal of Hydrogen Energy* **47**, 27383 (2022).
- [31] Z. Wang, H. Di, R. Sun, Y. Zhu, L. Yin, Z. Zhang, and C. Wang, Electrocatalytic Hydrogen Evolution Performance of Modified Ti₃C₂O₂ Doped with Non-metal Elements: A DFT Study, *ChemPhysMater* **1**, 321 (2022).
- [32] S. Ma, X. Fan, Y. An, D. Yang, Z. Luo, Y. Hu, and N. Guo, Exploring the Catalytic Activity of MXenes M_{n+1}C_nO₂ for Hydrogen Evolution, *Journal of Materials Science* **54** (2019).
- [33] V. Wiki, [Retrieved on 18th January,2025], https://www.vasp.at/wiki/index.php/Computing_the_work_function.
- [34] H. Radinger, V. Trouillet, F. Bauer, and F. Scheiba, Work function describes the electrocatalytic activity of graphite for vanadium oxidation, *ACS Catalysis* **12**, 6007–6015 (2022).
- [35] F. Calle-Vallejo, M. T. M. Koper, and A. S. Bandarenka, Tailoring the catalytic activity of electrodes with monolayer amounts of foreign metals, *Chemical Society Reviews* **42**, 5210 (2013).
- [36] Z. Chen, T. Ma, W. Wei, W.-Y. Wong, C. Zhao, and B.-J. Ni, Work Function-Guided Electrocatalyst Design, *Advanced Materials* **36**, 2401568 (2024).
- [37] J. Pang, R. G. Mendes, A. Bachmatiuk, L. Zhao, H. Q. Ta, T. Gemming, H. Liu, Z. Liu, and M. H. Rummeli, Applications of 2D MXenes in Energy Conversion and Storage Systems, *Chem. Soc. Rev.* **48**, 72 (2019).
- [38] A. Sreedhar, Q. T. H. Ta, and J.-S. Noh, Versatile Role of 2D Ti₃C₂ MXenes for Advancements in the Photodetector Performance: A Review, *Journal of Industrial and Engineering Chemistry* **127**, 1 (2023).
- [39] S. K. Azadi, M. Zeynali, S. Asgharizadeh, and M. A. Fooladloo, Investigation of the optical and electronic properties of functionalized ti₃c₂ mxene with halid atoms using dft calculation, *Materials Today Communications* **35**, 106136 (2023).
- [40] J. Ran, G. Gao, F.-T. Li, T.-Y. Ma, A. Du, and S.-Z. Qiao, Ti₃C₂ MXene Co-catalyst on Metal Sulfide Photoabsorbers for Enhanced Visible-light Photocatalytic Hydrogen Production, *Nature Communications* **8**, 13907 (2017).
- [41] J. Jiang, F. Li, S. Bai, Y. Wang, K. Xiang, H. Wang, J. Zou, and J.-P. Hsu, Carbonitride MXene Ti₃CN(OH)_x@MoS₂ Hybrids as Efficient Electrocatalyst for Enhanced Hydrogen Evolution, *Nano Research* **16** (2022).
- [42] X. Wang, S. Huang, L. Deng, H. Luo, C. Li, Y. Xu, Y. Yan, and Z. Tang, Enhanced optical absorption of fe-, co- and

- ni-decorated Ti_3C_2 mxene: A first-principles investigation, *Physica E: Low-dimensional Systems and Nanostructures* **127**, 114565 (2021).
- [43] K. Gothandapani, G. Tamil Selvi, R. Sofia Jennifer, V. Velmurugan, S. Pandiaraj, M. Muthuramamoorthy, S. Pitchaimuthu, V. Raghavan, A. C. Josephine Malathi, A. Alodhayb, and A. Nirmala Grace, Ni- Ti_3C_2 mxene composite derived from ni-metal organic framework for electrochemical hydrogen evolution reaction in acidic and alkaline medium, *International Journal of Hydrogen Energy* **52**, 1164 (2024).
- [44] S. Kurth, M. Marques, and E. Gross, Density Functional Theory, in *Encyclopedia of Condensed Matter Physics*, Vol. 1 (Elsevier, 2005) pp. 395–399.
- [45] P. E. Blöchl, Projector Augmented-wave Method, *Phys. Rev. B* **50**, 17953 (1994).
- [46] G. Kresse and J. Hafner, Ab initio Molecular-dynamics Simulation of the Liquid-metal–Amorphous-semiconductor Transition in Germanium, *Phys. Rev. B* **49**, 14251 (1994).
- [47] G. Kresse and J. Furthmüller, Efficiency of Ab-initio Total Energy Calculations for Metals and Semiconductors Using a Plane-wave Basis Set, *Computational Materials Science* **6**, 15 (1996).
- [48] G. Kresse and J. Furthmüller, Efficient Iterative Schemes for Ab initio Total-energy Calculations using a Plane-wave Basis Set, *Phys. Rev. B* **54**, 11169 (1996).
- [49] G. Kresse and D. Joubert, From Ultrasoft Pseudopotentials to the Projector Augmented-wave Method, *Phys. Rev. B* **59**, 1758 (1999).
- [50] M. Ernzerhof and G. E. Scuseria, Assessment of the Perdew–Burke–Ernzerhof Exchange–Correlation Functional, *The Journal of Chemical Physics* **110**, 5029 (1999).
- [51] H. J. Monkhorst and J. D. Pack, Special Points for Brillouin-zone Integrations, *Phys. Rev. B* **13**, 5188 (1976).
- [52] T. Sakhraoui and F. Karlický, Electronic Nature Transition and Magnetism Creation in Vacancy-Defected Ti_2CO_2 MXene under Biaxial Strain: A DFTB + U Study, *ACS Omega* **7**, 42221 (2022).
- [53] R. Gebauer, Oxygen Vacancies in Zirconia and Their Migration: The Role of Hubbard-U Parameters in Density Functional Theory, *Crystals* **13**, 574 (2023).
- [54] M. Sahoo, A. Ray, and N. Singh, Theoretical Insights into the Hydrogen Evolution Reaction on VGe_2N_4 and NbGe_2N_4 Monolayers, *ACS Omega* **7**, 7837 (2022).
- [55] P. Sen, K. Alam, T. Das, R. Banerjee, and S. Chakraborty, Combinatorial Design and Computational Screening of Two-Dimensional Transition Metal Trichalcogenide Monolayers: Toward Efficient Catalysts for Hydrogen Evolution Reaction, *The Journal of Physical Chemistry Letters* **11**, 3192 (2020).
- [56] K. Huang, C. Li, H. Li, G. Ren, L. Wang, W. Wang, and X. Meng, Photocatalytic Applications of Two-Dimensional Ti_3C_2 MXenes: A Review, *ACS Applied Nano Materials* **3**, 9581 (2020).
- [57] Materials Project, <https://next-gen.materialsproject.org/materials/mp-1094034> (2025), Data retrieved from the Materials Project for Ti_3C_2 (mp-1094034) from database version v2024.12.18.
- [58] Materials Project, <https://next-gen.materialsproject.org/materials/mp-866083> (2025), Data retrieved from the Materials Project for Zr_3N_2 (mp-866083) from database version v2024.12.18.
- [59] B. S. Mohrdarghaemmaghami, A. Boochani, S. Mohammad Elahi, and H. Khosravi, The Vanadium Effect on the Electronic and Optical Properties of Ti_3C_2 Graphene like: Based DFT, *Results in Physics* **8** (2018).
- [60] A. Enyashin and A. Ivanovskii, Two-dimensional Titanium Carbonitrides and their Hydroxylated Derivatives: Structural, Electronic Properties and Stability of MXenes $\text{Ti}_3\text{C}_{2-x}\text{N}_x(\text{OH})_2$ from DFTB Calculations, *Journal of Solid State Chemistry* **207**, 42 (2013).
- [61] J. Kibsgaard, Z. Chen, B. Reinecke, and T. Jaramillo, Engineering the Surface Structure of MoS_2 to Preferentially Expose Active Edge Sites for Electrocatalysis, *Nature materials* **11**, 963 (2012).